

RESEARCH ARTICLE | FEBRUARY 12 2016

## Comparison of simplified sum-over-state expressions to calculate resonance Raman intensities including Franck-Condon and Herzberg-Teller effects

Julien Guthmuller



*J. Chem. Phys.* 144, 064106 (2016)

<https://doi.org/10.1063/1.4941449>



View  
Online



Export  
Citation

CrossMark

This article may be downloaded for personal use only. Any other use requires prior permission of the author and AIP Publishing. This article appeared in (citation of published article) and may be found at <https://doi.org/10.1063/1.4941449>


26 February 2024 10:24:00



**APL Quantum**  
Bridging fundamental quantum research with technological applications

**Now Open for Submissions**  
No Article Processing Charges (APCs) through 2024

**Submit Today**



# Comparison of simplified sum-over-state expressions to calculate resonance Raman intensities including Franck-Condon and Herzberg-Teller effects

Julien Guthmuller

Faculty of Applied Physics and Mathematics, Gdańsk University of Technology, Narutowicza 11/12, 80-233 Gdańsk, Poland

(Received 19 November 2015; accepted 26 January 2016; published online 12 February 2016)

Sum-over-state (SOS) expressions to simulate absorption spectroscopy and resonance Raman (RR) scattering including Franck-Condon (FC) and Herzberg-Teller (HT) effects are described. Starting from the general SOS method, several simplified SOS formulae are derived. In particular, within the so-called independent mode displaced harmonic oscillator model, it is shown that including the vibronic structure in the absorption and RR spectra only requires the calculation of FC overlap integrals of the type  $\langle \theta_{g0} | \theta_{ev} \rangle$ , where  $g$ ,  $e$ , and  $v$  stand for the electronic ground state, excited state, and vibrational quantum number, respectively. Additionally, an approximation of the latter approach is introduced, referred as the simplified  $\Phi_e$  method, in which the FC factors are neglected. This method is advantageous from the computational point of view and it is demonstrated that it reproduces the main characteristics of the more involved approaches. The merits and drawbacks of the different methods are discussed by applying them to the prototypical compound of Rhodamine 6G. Overall, this work intends to unravel and clarify some differences in the SOS theories of RR scattering. © 2016 AIP Publishing LLC. [<http://dx.doi.org/10.1063/1.4941449>]

## I. INTRODUCTION

The spectroscopy of resonance Raman (RR) scattering is a widely used technique, which has proven to be an excellent tool for unraveling the dynamics and structure of molecular excited states.<sup>1,2</sup> Indeed, RR spectroscopy probes the dynamics in the Franck-Condon (FC) region, which is generally short-lived and thus structurally similar to the ground state. The RR intensities, which are associated to the ground state vibrational frequencies, carry specific information about the structure of the resonant electronic states. For example, identification of the vibrational modes with strong RR enhancements is used in multichromophoric systems to determine the chromophore involved in the excitation at a certain frequency and to assign the type of the electronic transitions. Additionally, the enhancement pattern reflects the geometric and electronic structures of the excited state. Therefore, RR intensity analysis is employed to elucidate the displacements of potential energy surfaces (PESs) of excited states relative to the ground state to extract changes in bond lengths upon electronic excitation and to calculate reorganization energies, e.g., for charge transfer processes.<sup>3–6</sup>

The interpretation of experimental RR spectra can strongly benefit from accurate calculations of the RR intensities, which can be obtained from the Kramers, Heisenberg, and Dirac expression of the Raman polarizability tensor.<sup>7,8</sup> To this aim, several methodologies were proposed recently in the literature, which can be classified into two families. The first type of method is based on an explicit evaluation of the sum-over-state (SOS) expression for the Raman polarizability tensor. This type of method is also referred as time independent. The second type of method corresponds to a time dependent approach originally

developed by Heller and co-workers,<sup>9–12</sup> which is based on wave packet dynamics. In this formulation, the Raman polarizability is expressed as a half-Fourier transform of a time dependent overlap between the final and initial vibrational states. While time independent methods require the evaluation of an infinite summation over vibronic states, the time dependent formulation necessitates a numerical integration of an unbounded integral. Recent implementations and applications of the time dependent approach are discussed, e.g., in Refs. 13–18.

The purpose of the present work is to describe and assess several SOS methods to calculate RR intensities. This is motivated by the following facts: (i) SOS methods are employed by several research groups to compute RR intensities,<sup>19–28</sup> (ii) SOS methods are efficient and accurate in simulating RR spectra including large and complex molecular systems,<sup>29,30</sup> and (iii) several approximations/simplifications have appeared in the literature, which creates demand for an assessment of their respective merits. Therefore, the detailed derivation of different SOS expressions is presented in order to describe the involved approximations, to give the required input quantities, and to estimate their computational cost. The methods are applied to the well-known compound of Rhodamine 6G (R6G).<sup>31,32</sup> Thus, their ability in reproducing different physical effects is investigated. This concerns (i) the inclusion of non-Condon scattering, i.e., Herzberg-Teller (HT) effects, (ii) the dependence of the RR intensities with respect to the excitation frequency, (iii) the inclusion of Duschinsky rotation effects, and (iv) the reproduction of the vibronic structure in the absorption and RR excitation profiles. It is the author's intention that this contribution will help unraveling and clarifying some differences in the SOS theories of RR scattering.

The paper is organized as follows: Section II presents the main theory and the standard approximations used in absorption and RR spectroscopies. Section III provides the derivation of several simplified SOS approaches. Section IV describes the computational methods employed to calculate the properties of R6G. Section V reports and discusses the simulated absorption spectrum, RR intensities, and RR excitation profiles. Finally, conclusions are given in Section VI.

## II. THEORY AND MAIN APPROXIMATIONS

This section presents the definition of the absorption and RR cross sections as well as the main approximations employed to derive expressions for the FC and HT contributions. The formalism described in this section was already reported by different authors (see, e.g., Refs. 33, 24, 3, and 34) and is reproduced herein to introduce the employed notations as well as to make the document self-contained and intelligible to the reader.

### A. Absorption cross section

The absorption cross section for transitions from an initial state  $|i\rangle$  to an ensemble of final states  $|f\rangle$  is given by

$$\sigma_A(\omega_L) = \frac{4\pi^2}{3c\hbar} \omega_L \sum_f \sum_{\rho=\{x,y,z\}} |\langle i|\mu_\rho|f\rangle|^2 \frac{\Gamma}{\pi} \frac{1}{(\omega_{fi} - \omega_L)^2 + \Gamma^2}. \quad (1)$$

In Eq. (1),  $\omega_L$  is the frequency of the incident light,  $\langle i|\mu_\rho|f\rangle$  is a component of the transition dipole moment, and  $\omega_{fi} \equiv (E_f - E_i)/\hbar$  is the Bohr frequency between the initial ( $i$ ) and final ( $f$ ) states. A homogeneous broadening is described by a Lorentzian function with a damping factor  $\Gamma$ , i.e., the full width at half maximum (FWHM) is equal to  $2\Gamma$ .

In the following, it is assumed that the Born-Oppenheimer approximation is valid, that the vibrational modes and frequencies are obtained within the harmonic approximation, and that the transition occurs between the electronic ground state ( $g$ ) and an electronic excited state ( $e$ ) of the molecule. In this case, the initial and final vibronic states can be written as a product of the electronic  $|\phi\rangle$  and vibrational  $|\theta\rangle$  wave functions,

$$|i\rangle = |\phi_g\rangle|\theta_{gu}\rangle, \quad |f\rangle = |\phi_e\rangle|\theta_{ev}\rangle, \quad (2)$$

$u$  and  $v$  are multi-indices representing the harmonic quantum numbers of the vibrational normal modes of the ground and excited states, respectively, i.e.,  $u \equiv u_1, u_2, \dots, u_M$ , where  $M$  is the number of modes. Next, the transition dipole moment can be written as

$$\langle i|\mu_\rho|f\rangle = \langle \theta_{gu}|\langle \phi_g|\mu_\rho|\phi_e\rangle|\theta_{ev}\rangle = \langle \theta_{gu}|\mu_{\rho}_{ge}|\theta_{ev}\rangle, \quad (3)$$

where  $(\mu_\rho)_{ge}$  is a component of the electronic transition dipole moment between the electronic ground state and the electronic excited state.  $(\mu_\rho)_{ge}$  depends on the nuclear coordinates and can be developed as a Taylor series,

$$(\mu_\rho)_{ge} = (\mu_\rho)_{ge}^0 + \sum_l \left( \frac{\partial(\mu_\rho)_{ge}}{\partial Q_l} \right)_0 Q_l + \dots \quad (4)$$

$(\mu_\rho)_{ge}^0$  and  $(\partial(\mu_\rho)_{ge}/\partial Q_l)_0$  are, respectively, the electronic transition dipole moment and the derivative of the electronic transition dipole moment evaluated at the ground state equilibrium geometry (denoted by 0). The index  $l$  indicates a summation over all the mass-weighted normal coordinates  $Q_l$  of the ground state. An alternative choice is to expand the transition dipole moment with respect to the excited state normal coordinates.

The following steps are made in order to obtain an expression for the square modulus of the transition dipole moment  $|\langle i|\mu_\rho|f\rangle|^2$ :

- (i) Eq. (4) is truncated after the linear term with respect to  $Q_l$ . Then, it is reported in Eq. (3).
- (ii) The well-know identity for harmonic oscillators is employed,

$$\langle \theta_{gu}|Q_l|\theta_{ev}\rangle = \sqrt{\frac{\hbar}{2\omega_l}} \left\{ \sqrt{u_l} \langle \theta_{g\dots u_l-1\dots}|\theta_{ev}\rangle + \sqrt{u_l+1} \langle \theta_{g\dots u_l+1\dots}|\theta_{ev}\rangle \right\}, \quad (5)$$

where  $\omega_l$  is the vibrational frequency of the  $l$ th mode and  $\langle \theta_{gu}|\theta_{ev}\rangle$  denotes a FC integral describing the overlap between the vibrational wave functions of the ground state and excited state. Within the harmonic oscillator approximation, the FC overlap integrals are real quantities, i.e.,  $\langle \theta_{gu}|\theta_{ev}\rangle = \langle \theta_{ev}|\theta_{gu}\rangle$ .

- (iii) It is assumed herein that the initial state is in the vibrational ground state  $|\theta_{g0}\rangle$ , i.e.,  $u_l = 0 \forall l$ . However, the formalism can easily be generalized to describe temperature effects by including a Boltzmann distribution of initial states.
- (iv) The dimensionless vibrational coordinates  $q_l$  Eq. (6.1) are introduced. Additionally, simplified notations are employed for the transition dipole moment and its derivative Eqs. (6.2) and (6.3). In the following, it is also assumed that  $\mu_\rho$  and  $(\mu_\rho)'_l$  are real quantities,

$$q_l = \sqrt{\frac{\omega_l}{\hbar}} Q_l, \quad (6.1)$$

$$\mu_\rho \equiv (\mu_\rho)_{ge}^0, \quad (6.2)$$

$$(\mu_\rho)'_l \equiv \left( \frac{\partial(\mu_\rho)_{ge}}{\partial q_l} \right)_0 = \sqrt{\frac{\hbar}{\omega_l}} \left( \frac{\partial(\mu_\rho)_{ge}}{\partial Q_l} \right)_0. \quad (6.3)$$

After the steps (i)-(iv), the square modulus of the transition dipole moment can be written as

$$\begin{aligned} |\langle i|\mu_\rho|f\rangle|^2 &= (\mu_\rho)^2 \langle \theta_{g0}|\theta_{ev}\rangle^2 \\ &+ \sum_l \sqrt{2} \mu_\rho (\mu_\rho)'_l \langle \theta_{g1_l}|\theta_{ev}\rangle \langle \theta_{g0}|\theta_{ev}\rangle \\ &+ \sum_{l,l'} \frac{1}{2} (\mu_\rho)'_l (\mu_\rho)'_{l'} \langle \theta_{g1_l}|\theta_{ev}\rangle \langle \theta_{g1_{l'}}|\theta_{ev}\rangle. \end{aligned} \quad (7)$$

The notation  $|\theta_{g1_l}\rangle$  means that  $u_l = 1$  and  $u_i = 0 \forall i \neq l$ . Following the denomination introduced by Santoro *et al.*,<sup>35</sup> the

first, second, and third terms on the right-hand side of Eq. (7) describe the FC contribution, the FC/HT interference, and the pure HT contribution, respectively. The FC contribution involves the square of the transition dipole moment, the FC/HT contribution involves the products between the transition dipole moment  $\mu_\rho$  and the derivatives  $(\mu_\rho)'_l$  with respect to all normal coordinates, and the HT contribution involves all products of the type  $(\mu_\rho)'_l(\mu_\rho)'_{l'}$ .

## B. Resonance Raman cross section

The total and differential (for the commonly employed 90° scattering geometry) Raman cross sections for a transition between the initial  $|i\rangle$  and final  $|f\rangle$  vibronic states are given by<sup>1,2</sup>

$$\sigma_{i \rightarrow f} = \frac{\omega_L \omega_S^3}{18\pi \epsilon_0^2 c^4} \sum_{\rho, \sigma = \{x, y, z\}} |(\alpha_{\rho\sigma})'_{i \rightarrow f}|^2, \quad (8.1)$$

$$\frac{d\sigma_{i \rightarrow f}}{d\Omega} = \frac{\omega_L \omega_S^3}{16\pi^2 \epsilon_0^2 c^4} \frac{1}{45} (45a^2 + 5\delta^2 + 7\gamma^2), \quad (8.2)$$

where  $\omega_L$  is the frequency of the incident light,  $\omega_S$  is the frequency of the scattered light, and  $a^2$ ,  $\delta^2$ , and  $\gamma^2$  are the three Raman invariants for randomly oriented molecules (see the supplementary material<sup>36</sup>), which depend on the Raman polarizability tensor  $(\alpha_{\rho\sigma})_{i \rightarrow f}$ ,

$$(\alpha_{\rho\sigma})_{i \rightarrow f} = \frac{1}{\hbar} \sum_k \left\{ \frac{\langle f | \mu_\rho | k \rangle \langle k | \mu_\sigma | i \rangle}{\omega_{ki} - \omega_L - i\Gamma} + \frac{\langle f | \mu_\sigma | k \rangle \langle k | \mu_\rho | i \rangle}{\omega_{kf} + \omega_L + i\Gamma} \right\}. \quad (9)$$

The index  $k$  indicates a summation over all the vibronic states of the molecule.

The following approximations are introduced.

- (i) In Eq. (9), only the first “resonant” term is kept, while the second “non-resonant” term is neglected. This is a good approximation for an excitation frequency  $\omega_L$  in close resonance with a set of vibronic states  $|k\rangle$  ( $\omega_L \approx \omega_{ki}$ ).
- (ii) The Born-Oppenheimer and harmonic oscillator approximations are employed.
- (iii) The transition dipole moments are expanded in a Taylor series up to the second term according to Eq. (4).
- (iv) Only RR intensities for fundamental transitions are considered herein, i.e., the initial state is  $|\phi_g\rangle|\theta_{g0}\rangle$  and the final state is  $|\phi_g\rangle|\theta_{g1n}\rangle$ .

Under approximations (i)-(iv), the RR polarizability tensor can be written in the form

$$(\alpha_{\rho\sigma})_{g0 \rightarrow g1n} = \frac{1}{\hbar\sqrt{2}} \sum_{e \neq g} \left\{ (FC)_e^{RR} + (FC/HT)_e^{RR} + (HT)_e^{RR} \right\}, \quad (10)$$

where  $(FC)_e^{RR}$ ,  $(FC/HT)_e^{RR}$ , and  $(HT)_e^{RR}$  are the FC, the FC/HT, and the HT contributions to the Raman polarizability tensor, respectively. The index  $e$  indicates a summation over all the resonant excited states ( $e$ ). The derivation of Eqs. (10) and (11) made use of the identity of Eq. (5) and of the notations introduced in Eqs. (6),

$$(FC)_e^{RR} = \sqrt{2} \mu_\rho \mu_\sigma \sum_v \frac{\langle \theta_{g1n} | \theta_{ev} \rangle \langle \theta_{g0} | \theta_{ev} \rangle}{\omega_{eg} + \omega_{v0} - \omega_L - i\Gamma}, \quad (11.1)$$

$$(FC/HT)_e^{RR} = \mu_\rho \sum_l (\mu_\sigma)'_l \sum_v \frac{\langle \theta_{g1n} | \theta_{ev} \rangle \langle \theta_{g1l} | \theta_{ev} \rangle}{\omega_{eg} + \omega_{v0} - \omega_L - i\Gamma} + (\mu_\rho)'_n \mu_\sigma \sum_v \frac{[\langle \theta_{g0} | \theta_{ev} \rangle + \sqrt{2} \langle \theta_{g2n} | \theta_{ev} \rangle] \langle \theta_{g0} | \theta_{ev} \rangle}{\omega_{eg} + \omega_{v0} - \omega_L - i\Gamma} + \sum_{l \neq n} (\mu_\rho)'_l \mu_\sigma \sum_v \frac{\langle \theta_{g1n1l} | \theta_{ev} \rangle \langle \theta_{g0} | \theta_{ev} \rangle}{\omega_{eg} + \omega_{v0} - \omega_L - i\Gamma}, \quad (11.2)$$

$$(HT)_e^{RR} = \sum_l (\mu_\rho)'_n (\mu_\sigma)'_l \frac{1}{\sqrt{2}} \sum_v \frac{[\langle \theta_{g0} | \theta_{ev} \rangle + \sqrt{2} \langle \theta_{g2n} | \theta_{ev} \rangle] \langle \theta_{g1l} | \theta_{ev} \rangle}{\omega_{eg} + \omega_{v0} - \omega_L - i\Gamma} + \sum_{l \neq n} \sum_{l'} (\mu_\rho)'_l (\mu_\sigma)'_{l'} \frac{1}{\sqrt{2}} \sum_v \frac{\langle \theta_{g1n1l} | \theta_{ev} \rangle \langle \theta_{g1l'} | \theta_{ev} \rangle}{\omega_{eg} + \omega_{v0} - \omega_L - i\Gamma}, \quad (11.3)$$

where  $\omega_{eg}$  and  $\omega_{v0}$  describe the electronic and vibrational transition frequencies, respectively. The index  $v$  indicates a summation over all the vibrational states (described by the harmonic quantum numbers  $\equiv v_1, v_2, \dots, v_M$ ) of the electronic state ( $e$ ). The notation  $|\theta_{g1n1l}\rangle$  means that  $u_n = 1$ ,  $u_l = 1$ , and  $u_i = 0 \forall i \neq n, l$ .

## III. SUM-OVER-STATE EXPRESSIONS IN THE FRAME OF THE INDEPENDENT MODE DISPLACED HARMONIC OSCILLATOR (IMDHO) MODEL

The simulation of absorption and RR spectra requires the calculation of the square modulus of the transition dipole

moment (Eq. (7)) and of the RR transition polarizability tensor (Eq. (10)), respectively. This demands the computation of the electronic transition frequencies  $\omega_{eg}$  (i.e., adiabatic transition energies), vibrational transition frequencies  $\omega_{v0}$  (i.e., harmonic vibrational frequencies), components of the transition dipole moment  $\mu_\rho$ , and their derivatives  $(\mu_\rho)'_l$ . These quantities can be obtained from quantum chemistry calculations making use of density functional theory (DFT) or wave function based approaches. Additionally, it is necessary to evaluate the FC overlap integrals between the ground state ( $g$ ) and the excited states ( $e$ ). In the general case, in which the ground and excited states have different equilibrium geometries, different vibrational frequencies, and different normal coordinates (i.e., inclusion of Duschinsky rotation effects), the FC overlap integrals can be computed using recursive relations.<sup>37</sup> This approach was applied to both absorption and RR spectra including or neglecting HT effects (see, e.g., Refs. 38, 31, 35, and 24). In particular, it requires the calculation of a large number of FC integrals, which can be classified according to the ground state ( $g$ ) vibrational state, i.e., values of the quantum number  $u$ . Hence, integrals of the type  $\langle\theta_{g0}|\theta_{ev}\rangle$  and  $\langle\theta_{g1n}|\theta_{ev}\rangle$  are necessary to calculate the absorption spectrum (Eq. (7)) as well as the RR intensities within the FC approximation. In addition, integrals of the type  $\langle\theta_{g2n}|\theta_{ev}\rangle$  and  $\langle\theta_{g1n1l}|\theta_{ev}\rangle$  are required to simulate the RR spectrum including HT effects. An accurate evaluation of the absorption cross section and of the RR transition polarizability demands convergence of the—in principle infinite—summations over  $v$  (Eqs. (1) and (10)), which involve products of FC integrals of the type  $\langle\theta_{gu}|\theta_{ev}\rangle\langle\theta_{gu'}|\theta_{ev}\rangle$ . This task requires consideration of a large number of vibrational states ( $u$ ,  $u'$ , and  $v$ ), which may lead to convergence difficulties (i.e., a proper set of vibrational states  $v$  need to be selected) as well as to a higher computational burden for large molecules or when several electronic excited states need to be included. Therefore, even if efficient algorithms were implemented recently to perform such summations,<sup>24</sup> it is of interest to introduce additional approximations to reduce the computational cost and to overcome possible problems in the evaluation of the summations. The purpose of this section is to introduce some simplified expressions to simulate absorption and RR spectra. Next, in Secs. IV and V, these expressions will be applied on a typical model compound and compared to one another.

The most widely employed and simplest approximation to describe the PESs of the ground and excited states is known as the IMDHO model, in which it is assumed that the ground and excited states share the same normal coordinates (neglect of Duschinsky rotation) and the same vibrational frequencies. This model was applied to many molecular systems and provided in several cases a sufficiently accurate description of the excited states PESs allowing a reproduction of the RR intensities and an assignment of experimental bands (see, e.g., Refs. 19, 32, and 29). In this case, the difference between the ground and excited states ( $e$ ) PESs is only determined by the dimensionless displacements  $\Delta_{e,l}$  along the normal coordinates ( $l$ ). Within the IMDHO model, the multidimensional FC integrals  $\langle\theta_{gu}|\theta_{ev}\rangle$  can be written as a product of one dimensional FC integrals and simple recursive

relations<sup>39</sup> can be used to compute them efficiently (see the supplementary material<sup>36</sup>).

As presented below (Sections III A and III B), an interesting feature of the IMDHO model resides in the fact that it is possible to derive expressions for the absorption cross section and RR polarizability tensor that depend only on the FC integrals of the type  $\langle\theta_{g0}|\theta_{ev}\rangle$ . Therefore, the use of such expressions only requires the calculation of a set of FC integrals (defined by the quantum numbers  $v$ ), so that the sum of FC factors  $\sum_v \langle\theta_{g0}|\theta_{ev}\rangle^2$  converges to unity. This makes the approach computationally attractive as integrals of the types  $\langle\theta_{g1n}|\theta_{ev}\rangle$ ,  $\langle\theta_{g2n}|\theta_{ev}\rangle$ , and  $\langle\theta_{g1n1l}|\theta_{ev}\rangle$  do not need to be explicitly calculated. A further advantage of these expressions is that they can be used as a starting point to introduce additional approximations leading to simplified sum-over-state expressions (Sections III C and III D).

## A. Absorption

Starting from Eqs. (1) and (7), and making use of recursive relations for the FC overlap integrals, the absorption cross section can be written as

$$\sigma_A(\omega_L) = \frac{4\pi}{3c\hbar} \omega_L \sum_{e \neq g} \left\{ (FC)_e^A + (FC/HT)_e^A + (HT)_e^A \right\}, \quad (12)$$

where

$$(FC)_e^A = \sum_{\rho=\{x,y,z\}} \mu_\rho \mu_\rho \text{Im}\{\Phi_e(\omega_L)\}, \quad (13.1)$$

$$(FC/HT)_e^A = \sum_l \sum_{\rho=\{x,y,z\}} \mu_\rho (\mu_\rho)'_l \Delta_l \text{Im}\{\Phi_e(\omega_L) - \Phi_e(\omega_L - \omega_l)\}, \quad (13.2)$$

$$(HT)_e^A = \sum_l \sum_{\rho=\{x,y,z\}} (\mu_\rho)'_l (\mu_\rho)'_l \frac{1}{2} \text{Im}\{\Phi_e(\omega_L - \omega_l)\} + \sum_{l,l'} \sum_{\rho=\{x,y,z\}} (\mu_\rho)'_l (\mu_\rho)'_{l'} \frac{\Delta_l \Delta_{l'}}{4} \text{Im}\{\Phi_e(\omega_L) - \Phi_e(\omega_L - \omega_l) - \Phi_e(\omega_L - \omega_{l'}) + \Phi_e(\omega_L - \omega_l - \omega_{l'})\}. \quad (13.3)$$

The function  $\Phi_e(\omega_L)$  is defined as<sup>40,19</sup>

$$\Phi_e(\omega_L) \equiv \sum_v \frac{\langle\theta_{g0}|\theta_{ev}\rangle^2}{\omega_{eg} + \omega_{v0} - \omega_L - i\Gamma}. \quad (14)$$

To simplify the notations, the dimensionless displacements for the excited state ( $e$ ) are defined as  $\Delta_l \equiv \Delta_{e,l}$ .

## B. Resonance Raman

Following a similar approach, the three terms appearing in Eq. (10) for the definition of the RR polarizability tensor can be written as



$$(FC)_e^{RR} = \mu_\rho \mu_\sigma \Delta_n \{ \Phi_e(\omega_L) - \Phi_e(\omega_L - \omega_n) \}, \quad (15.1)$$

$$(FC/HT)_e^{RR} = \mu_\rho (\mu_\sigma)'_n \Phi_e(\omega_L - \omega_n) + (\mu_\rho)'_n \mu_\sigma \Phi_e(\omega_L) + \sum_l \{ \mu_\rho (\mu_\sigma)'_l + (\mu_\rho)'_l \mu_\sigma \} \frac{\Delta_n \Delta_l}{2} \{ \Phi_e(\omega_L) - \Phi_e(\omega_L - \omega_n) - \Phi_e(\omega_L - \omega_l) + \Phi_e(\omega_L - \omega_n - \omega_l) \}, \quad (15.2)$$

$$(HT)_e^{RR} = \sum_l (\mu_\rho)'_l (\mu_\sigma)'_n \frac{\Delta_l}{2} \{ \Phi_e(\omega_L - \omega_n) - \Phi_e(\omega_L - \omega_n - \omega_l) \} + \sum_l (\mu_\rho)'_l (\mu_\sigma)'_l \frac{\Delta_n}{2} \{ \Phi_e(\omega_L - \omega_l) - \Phi_e(\omega_L - \omega_n - \omega_l) \} + \sum_l (\mu_\rho)'_n (\mu_\sigma)'_l \frac{\Delta_l}{2} \{ \Phi_e(\omega_L) - \Phi_e(\omega_L - \omega_l) \} + \sum_{l,l'} (\mu_\rho)'_l (\mu_\sigma)'_{l'} \frac{\Delta_n \Delta_l \Delta_{l'}}{4} \{ \Phi_e(\omega_L) - \Phi_e(\omega_L - \omega_n) - \Phi_e(\omega_L - \omega_l) - \Phi_e(\omega_L - \omega_{l'}) + \Phi_e(\omega_L - \omega_n - \omega_l) + \Phi_e(\omega_L - \omega_n - \omega_{l'}) + \Phi_e(\omega_L - \omega_l - \omega_{l'}) - \Phi_e(\omega_L - \omega_n - \omega_l - \omega_{l'}) \}. \quad (15.3)$$

The derivation of Eqs. (12)–(15) presents no particular difficulties but is too tedious to be fully described here. The interested reader can find details on the derivation in the supplementary material.<sup>36</sup> Despite rather lengthy expressions, Eqs. (13) and (15) can easily be implemented in programs and evaluated by computers. Indeed, they involve only finite summations over the vibrational modes ( $l$ ), in which the summands are products between the transition dipole moments, their derivatives, the dimensionless displacements, and a linear combination of the  $\Phi_e$  function evaluated at different frequencies. The interesting features are that the summation over the FC integrals (described by the quantum numbers  $v$ ) is moved in the definition of the  $\Phi_e$  function and as stated before only involves FC integrals of the type  $\langle \theta_{g0} | \theta_{ev} \rangle$ . As shown by Eqs. (13) and (15), these properties are verified both when FC and HT effects are included. The formalism employed in Sections III A and III B originates from the transform theory.<sup>41,40,42,43</sup> In particular, the FC contributions (Eqs. (13.1) and (15.1)) as well as the two first terms of the FC/HT contribution (Eq. (15.2)) were already reported in the literature.<sup>43,44</sup> However, to the author's knowledge, the full expressions for the FC/HT and HT contributions of absorption and RR are presented for the first time using this formulation and are applied in Section V to compute HT effects.

### C. Simplified $\Phi_e$ function

The expressions reported in Secs. III A and III B allow the computation of the absorption and RR intensities. In particular, they require the calculation of the adiabatic transition frequency  $\omega_{eg}$  as well as the FC factors  $\langle \theta_{g0} | \theta_{ev} \rangle^2$ . However, in some cases it can be computationally advantageous to avoid calculating the FC factors and to replace the determination of the adiabatic transition frequency by the calculation of the vertical transition frequency, denoted  $\Omega_{eg}$ . This can be performed by virtue of the FC principle, which states that the most probable transition (given by the FC factor) occurs

vertically from the ground state geometry. Therefore, the values of  $\omega_{eg} + \omega_{v0}$  in Eq. (14) can be approximated by the vertical transition frequency ( $\Omega_{eg}$ ). Application of this simplification along with the property that  $\sum_v \langle \theta_{g0} | \theta_{ev} \rangle^2 = 1$  leads to

$$\Phi_e(\omega_L) \cong \frac{1}{\Omega_{eg} - \omega_L - i\Gamma}. \quad (16)$$

A particular case of the latter simplification is known as the small shift approximation<sup>33</sup> for RR intensities, in which the geometrical displacements are assumed to be small. In this situation, the largest FC factor is given by  $\langle \theta_{g0} | \theta_{e0} \rangle^2$ , meaning that the adiabatic and vertical transition frequencies almost coincide (see the supplementary material<sup>36</sup> for the connection between the small shift approximation and the simplified  $\Phi_e$  function approach).

The  $\Phi_e$  function was originally defined within the frame of the transform theory. This theory uses the fact that, within the FC approximation, the absorption spectrum is related to the imaginary part of the  $\Phi_e$  function (see Eq. (13.1)). Hence, employing the experimental absorption spectrum and its Kramers-Kronig transform, RR excitation profiles can be simulated. In the present work, the  $\Phi_e$  function is directly evaluated from the SOS expression (Eqs. (14) and (16)) without making direct use of the experimental spectrum. Nevertheless, the connection between the  $\Phi_e$  function and the absorption spectrum gives an indication that the simplified  $\Phi_e$  function approximation should be valid in situations when the excitation frequency  $\omega_L$  is in resonance with absorption bands displaying a large broadening and non-resolved vibronic structure. It should be mentioned that the present formulation neglects inhomogeneous broadening effects, which might be predominant for experiments done, e.g., in solution. Such effects can be easily included (see, e.g., Ref. 45). For example, the simplified  $\Phi_e$  function approximation was employed recently in several applications on transition metal complexes

and succeeded in reproducing the main characteristics of RR spectra.<sup>45,29,46</sup>

#### D. Simplified SOS

In the case of RR spectroscopy, several authors extended to use of the Placzek and double harmonic approximations to obtain RR intensities directly from the derivatives of the frequency dependent polarizability with respect to the normal coordinates.<sup>47–49</sup> In particular, Rappoport *et al.*<sup>27</sup> derived a simplified SOS expression including FC and HT contributions. Using a similar nomenclature as in Eqs. (15), the simplified SOS formula reads

$$(FC)_e^{RR} = -\mu_\rho \mu_\sigma \left( \frac{\partial \Omega_{eg}}{\partial q_n} \right)_0 \times \left\{ \frac{(\Omega_{eg} - \omega_L)^2 - \Gamma^2 + 2i\Gamma(\Omega_{eg} - \omega_L)}{[(\Omega_{eg} - \omega_L)^2 + \Gamma^2]^2} \right\}, \quad (17.1)$$

$$(FC/HT)_e^{RR} = \{ \mu_\rho (\mu_\sigma)'_n + (\mu_\rho)'_n \mu_\sigma \} \left\{ \frac{\Omega_{eg} - \omega_L + i\Gamma}{(\Omega_{eg} - \omega_L)^2 + \Gamma^2} \right\}. \quad (17.2)$$

A derivation of the expression and the connection with the simplified  $\Phi_e$  function approximation is provided in the supplementary material.<sup>36</sup> The advantage of this formula is that it is easily computed and that it requires only quantities calculated at the ground state geometry, namely, the vertical transition frequencies ( $\Omega_{eg}$ ) and their derivatives ( $\partial \Omega_{eg} / \partial q_l$ )<sub>0</sub> and the transition dipole moments ( $\mu_\rho$ ) and their derivatives ( $\mu_\rho$ )'\_l.

Within the IMDHO model, the gradients ( $\partial \Omega_{eg} / \partial q_l$ )<sub>0</sub> can be related to the dimensionless displacements according to

$$\Delta_l = -\frac{1}{\omega_l} \left( \frac{\partial \Omega_{eg}}{\partial q_l} \right)_0. \quad (18)$$

Using this relation, it can be shown that the simplified SOS formula (Eq. (17)) is an approximation of the simplified  $\Phi_e$  function approach. As presented in the supplementary material,<sup>36</sup> it approximates the dependence on the excitation frequency ( $\omega_L$ ) for the FC and FC/HT contributions, and it neglects part of the FC/HT contribution and totally the HT contribution. In particular, concerning the FC/HT contribution, the simplified SOS approximation leads to a symmetric polarizability tensor with respect to exchange of the  $\rho$  and  $\sigma$  components. Therefore, it cannot describe anomalous polarization effects.<sup>33</sup>

#### E. Summary of SOS methods for RR intensities

The different SOS approaches presented in this work are summarized in Fig. 1. The methods are ordered starting from the simplest and computationally cheapest (given at the bottom of the ladder) to the more involved and computationally demanding (top of the ladder). For each method, the required quantities are also reported. Note that in all cases, calculation of the ground state vibrational frequencies and normal coordinates is necessary.

Method	Required quantities
Full SOS Eq. (11) Duschinsky FC, FC/HT, HT	$\mu_\rho$ ( $\mu_\rho$ )'_l, $\omega_{eg}$ , $\Delta_l$ , $\langle \theta_{g0}   \theta_{ev} \rangle$ $\langle \theta_{g1}   \theta_{ev} \rangle$ , $\langle \theta_{g2}   \theta_{ev} \rangle$ , $\langle \theta_{g1,1}   \theta_{ev} \rangle$ Excited state Hessian
IMDHO Model Eqs. (15, 14) FC, FC/HT, HT	$\mu_\rho$ ( $\mu_\rho$ )'_l, $\omega_{eg}$ , $\Delta_l$ , $\langle \theta_{g0}   \theta_{ev} \rangle$
Simplified $\Phi_e$ Eqs. (15, 16) FC, FC/HT, HT	$\mu_\rho$ ( $\mu_\rho$ )'_l, $\Omega_{eg}$ , $\Delta_l$
Simplified SOS Eq. (17) FC, FC/HT	$\mu_\rho$ ( $\mu_\rho$ )'_l, $\Omega_{eg}$ , $\left( \frac{\partial \Omega_{eg}}{\partial q_l} \right)_0$
ST Eq. (19) FC	$\left( \frac{\partial \Omega_{eg}}{\partial q_l} \right)_0$

Computational cost

FIG. 1. Ladder of SOS methods to calculate RR intensities.

At the bottom of the ladder is the most widely employed and simplest method to calculate relative RR intensities. This approach is known as the short-time (ST) approximation<sup>9</sup> or simply as the gradient method. It includes only FC effects and the approach can be used when a single electronic excited state is in resonance with the excitation frequency ( $\omega_L$ ). Thus, the relative RR intensities for fundamental transitions are given by

$$I_{g0 \rightarrow g1n} \propto \left( \frac{\partial \Omega_{eg}}{\partial q_l} \right)_0^2. \quad (19)$$

The next rung of the ladder describes the simplified SOS method. This approach neglects the vibronic structure in the RR excitation profile and requires only vertical quantities, namely, the excitation frequencies, the transition dipole moments, and their derivatives. The simplified SOS method is an approximation of the simplified  $\Phi_e$  approach. In the latter approach, the displacements can be calculated from the excited state gradients (Eq. (18)), which makes the simplified  $\Phi_e$  method equivalent to the simplified SOS method in terms of the input data and of the computational cost, but not in terms of the results (see Section V). An alternative way is to calculate the displacements from the difference between the excited states and ground state geometries. This is often called the adiabatic shift method (see, e.g., Refs. 24, 26, 18, and 50), in which an optimization of the excited state geometries is necessary. The next rung corresponds to the IMDHO model. In the formulation of Eqs. (15) and (14), this model only requires—in addition to the simplified  $\Phi_e$  input data—the calculation of FC integrals of the type  $\langle \theta_{g0} | \theta_{ev} \rangle$  as well as an estimation of the adiabatic transition frequency ( $\omega_{eg}$ ). This makes the model computationally advantageous over the more involved full SOS approach, which requires the calculation of

additional types of FC integrals. The full SOS method also includes Duschinsky rotation effects and hence necessitates the calculation of the excited state Hessian.

As mentioned in recent works,<sup>26,18</sup> the main computational burden is associated to the calculation of the required quantities by quantum chemistry methods. In particular, the computation of the displacements in the adiabatic shift method or of the excited state Hessian in the full SOS method is more time consuming. Calculation of the derivatives of the transition dipole moments has also an important computational cost when done by numerical differentiation. Usually, the calculation of the FC integrals and of the RR cross sections represents only a small fraction of the total computational cost. Nevertheless, the use of simplified approaches like the IMDHO model or the simplified  $\Phi_e$  method makes the evaluation of the RR cross section easier and it can avoid possible inaccuracies arising from the incomplete convergence of the summation of FC integrals.

#### IV. COMPUTATIONAL METHODS

Quantum chemical calculations were performed with the GAUSSIAN 09 program,<sup>51</sup> which provides the structural and electronic data necessary for the simulation of the absorption and RR spectra of the R6G molecule. All the calculations were performed in a vacuum by means of DFT and time dependent DFT (TDDFT) using the B3LYP exchange-correlation functional with the 6-311G(d) basis set. These methods were proven to be accurate for the simulation of the RR spectrum of R6G<sup>31,32</sup> in resonance with the first singlet excited state  $S_1$ . The geometry, harmonic vibrational frequencies, and normal coordinates of the ground state  $S_0$  were obtained by DFT, whereas the vertical excitation energies and transition dipole moments of the  $S_1$  excited state were obtained by TDDFT. The geometry and harmonic vibrations of the  $S_1$  state were also computed with TDDFT in order to investigate Duschinsky rotation effects. To correct for the lack of anharmonicity and the approximate treatment of electron correlation, the harmonic frequencies were scaled by the factor 0.98.

A program developed locally is employed to calculate the RR cross sections and absorption spectra. In particular, this demands the computation of the geometrical displacements  $\Delta_l$ , derivatives of the transition dipole moment  $(\mu_\rho)_l'$ , and FC overlap integrals  $\langle \theta_{gu} | \theta_{ev} \rangle$ . Within the IMDHO model, the displacements were calculated from the gradients (Eq. (18)) as well as by projecting the difference between the  $S_1$  and  $S_0$  geometries on the ground state normal coordinates (adiabatic shift method). The latter displacements were also employed to compute absorption and RR spectra in association with Duschinsky effects (adiabatic Hessian method<sup>24</sup>). The FC overlap integrals were computed from the displacements, vibrational frequencies, and normal coordinates using recursive relations.<sup>37</sup> Within the IMDHO model, a nearly complete convergence of the FC factor summation was obtained, with a value of  $\sum_v \langle \theta_{g0} | \theta_{ev} \rangle^2 > 0.99$ . When Duschinsky effects are included, the summations of the FC overlap integrals were not completely converged, e.g., the summation of the FC factors  $\sum_v \langle \theta_{g0} | \theta_{ev} \rangle^2$  reaches a value of only 0.92. This incomplete

convergence leads to an underestimation of the absolute RR cross sections but has only a weak impact on the relative RR intensities and on the shapes of the excitation profiles (see Section V). The derivatives  $(\partial \Omega_{eg} / \partial q_l)_0$  and  $(\mu_\rho)_l'$  were obtained by a two-point numerical differentiation procedure from the vertical excitation energies and transition dipole moments, which were computed with TDDFT for distorted structures resulting from the addition or subtraction of a finite displacement along the normal coordinates to the ground state geometry. In the simulation of the absorption and RR spectra, a value of  $\Gamma$  equal to  $400 \text{ cm}^{-1}$  was assumed to reproduce the experimental broadening<sup>52</sup> and the transition frequency had been shifted so that the experimental (530 nm) and theoretical absorption maxima  $\lambda_{max}$  coincided, namely, a  $\omega_{eg}$  of  $18\,800 \text{ cm}^{-1}$  was employed with the full SOS and IMDHO model methods, whereas a  $\Omega_{eg}$  of  $18\,867 \text{ cm}^{-1}$  was employed when using the simplified  $\Phi_e$  and simplified SOS approximations. The RR spectra were simulated for an excitation wavelength of 532 nm (i.e.,  $\omega_L$  of  $18\,797 \text{ cm}^{-1}$ ) and a Lorentzian function with a FWHM of  $5 \text{ cm}^{-1}$  was employed to broaden the Raman intensities.

#### V. APPLICATION TO RHODAMINE 6G

The methods described in Secs. I–IV to simulate absorption and RR spectroscopies are applied to the prototypical compound of Rhodamine 6G. The RR properties of this dye were investigated in the past both from the theoretical and experimental points of view.<sup>31,32,16,52</sup> In particular, important vibronic effects were identified in the RR spectrum for excitation frequencies close to the absorption maximum. Therefore, it constitutes a good example on which the different SOS approximations can be tested and on which their effects can be discussed.

##### A. Absorption spectra

The vibronic structure of the absorption spectrum for the first singlet excited state ( $S_1$ ) was simulated according to Eq. (1). The results obtained in the FC approximation are presented at the top of Fig. 2 and made use of three different methods. Within the IMDHO model, the displacements were calculated from the gradients as well as from the difference between the  $S_1$  and  $S_0$  geometries. Additionally, the spectrum including Duschinsky effects was simulated. As discussed in previous works,<sup>31,32</sup> the spectrum is dominated by a single band with a vibronic shoulder at higher energy. Fig. 2 shows that the spectra obtained from the gradients and from the geometry difference are superimposed. This indicates that in this case, the gradient approximation is appropriate to calculate the geometrical displacements. The inclusion of Duschinsky rotation effects leads to a transfer of intensity from the maximum of absorption to the vibronic shoulder. Nevertheless, the change of vibrational frequencies between the ground and excited states as well as the effect of Duschinsky mixing remains rather limited in the present system. Therefore, all methods are in overall agreement with the experimental spectrum.<sup>52</sup>



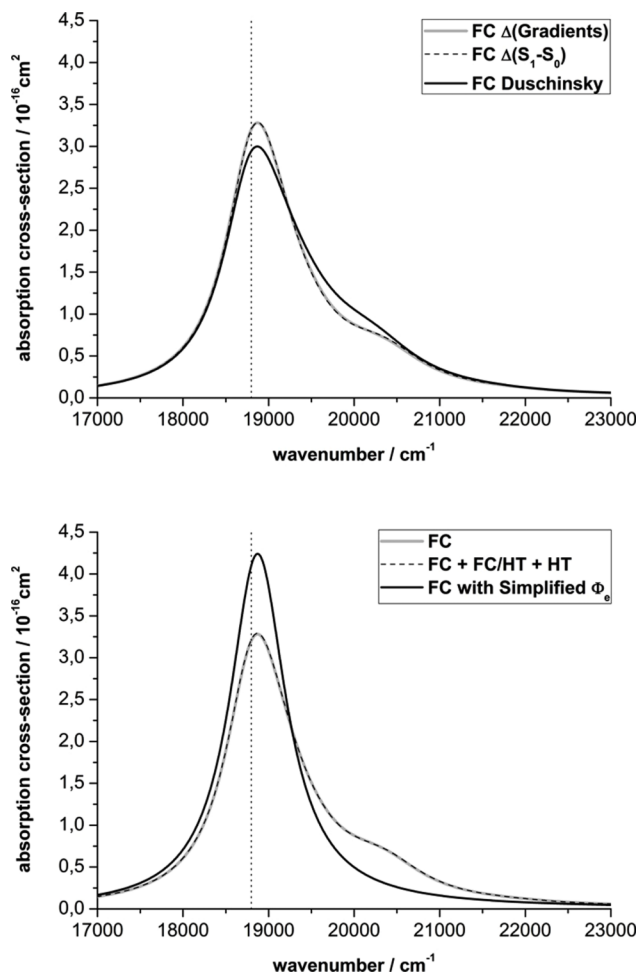


FIG. 2. Top: Comparison between the absorption spectra calculated in the FC approximation.  $\Delta$ 's obtained from the gradients within the IMDHO model (grey line),  $\Delta$ 's obtained from the difference between the  $S_1$  and  $S_0$  geometries within the IMDHO model (dashed line) and including Duschinsky rotation effects (black line). Bottom: Absorption spectra calculated within the IMDHO model with  $\Delta$ 's obtained from the gradients. In the FC approximation (grey line), including FC, FC/HT, and HT terms (dashed line) and including only the FC contribution with the simplified  $\Phi_e$  method (black line). The vertical dotted line indicates the excitation frequency employed in Section V B.

The bottom of Fig. 2 presents the absorption spectra calculated within the IMDHO model using gradients for the displacements. First, it is seen that the inclusion of the FC/HT and HT contributions is negligible for the absorption spectrum. This is the case within the IMDHO model (Fig. 2) and within the simplified  $\Phi_e$  method (results not shown). It can be related to the rather large oscillator strength of  $S_1$ , which has a calculated value of 0.744, indicating that the FC contribution dominates the spectrum. The use of the simplified  $\Phi_e$  approach leads to a single band in the absorption spectrum with no vibronic shoulder. This is related to the fact that in the FC approximation, the simplified  $\Phi_e$  method describes the absorption band by a single Lorentzian function (see Eqs. (13.1) and (16)). Therefore, in comparison to the IMDHO model, additional intensity is located close to the maximum of absorption. Because the simplified  $\Phi_e$  method neglects the vibronic structure in the absorption spectrum, it is only adequate to describe bands with small or negligible vibronic progressions. Additionally, this approximation is

also practical in situations when the structure of an absorption band is dominated by the contributions of several overlapping electronic excited states (see, e.g., Refs. 45 and 29). The effects of this simplification on the RR intensities and on the RR excitation profiles will be discussed in Secs. V B and V C. Inclusion of the FC/HT and HT contributions together with Duschinsky effects was not performed, but on the basis of the results obtained with the IMDHO model, it is expected that FC/HT and HT contributions will be also negligible in this case.

## B. RR spectra

In this section, the RR spectra obtained for an excitation frequency in close resonance with the maximum of absorption are described. The top of Fig. 3 considers the results calculated with the short-time approximation as well as with the IMDHO model including the FC contribution. Both methods provide

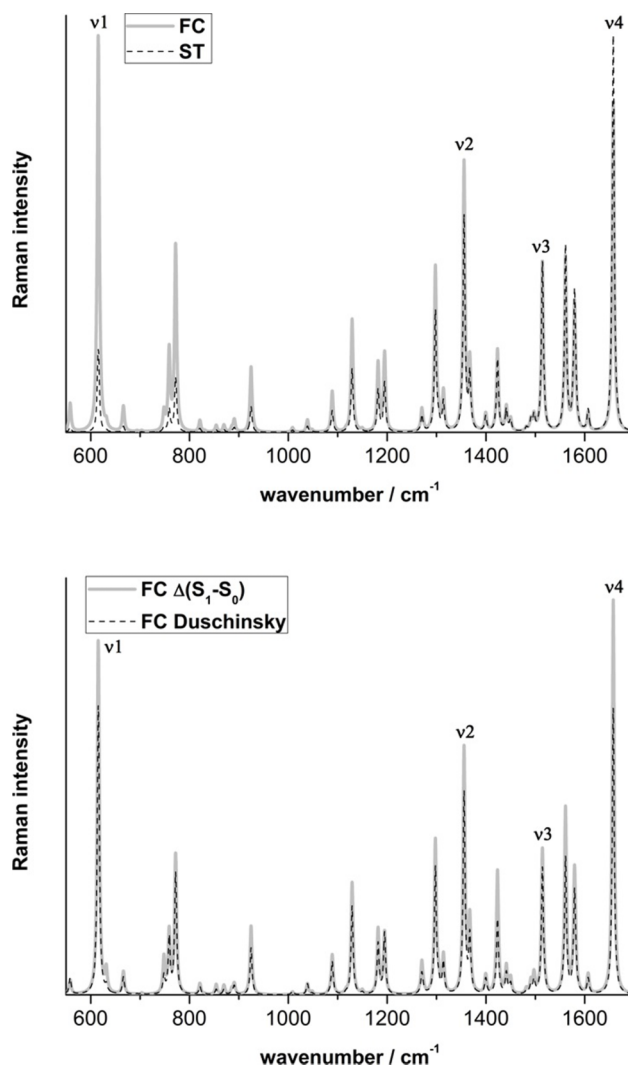


FIG. 3. Comparison between RR spectra obtained for an excitation in close resonance with the maximum of absorption. Top:  $\Delta$ 's obtained from the gradients in the FC approximation and within the IMDHO model (grey line) using the short-time approximation (dashed line). Bottom:  $\Delta$ 's obtained from the difference between the  $S_1$  and  $S_0$  geometries within the IMDHO model (grey line) and including Duschinsky rotation effects (dashed line) in the FC approximation. The four selected modes are indicated.

comparable relative intensities above  $1400\text{ cm}^{-1}$ , whereas the lower frequency modes have larger intensities using the IMDHO model. In particular, the large enhancement of the two vibrations at about  $610\text{ cm}^{-1}$  and  $770\text{ cm}^{-1}$  was ascribed to a vibronic effect,<sup>32</sup> which is not captured by the short-time approximation. The strong intensities of these two modes are in agreement with the experimental results<sup>52</sup> (see Fig. 4). Therefore, the short-time approximation is not fully adequate for simulating the RR spectrum of R6G in resonance with the first excited state.

The bottom of Fig. 3 presents the spectra calculated in the FC approximation using displacements computed from the geometry difference within the IMDHO model and including Duschinsky rotation effects (full SOS method). First, comparing with the top of Fig. 3, the IMDHO model gives some differences in the RR spectra when using displacements calculated from the gradients (Fig. 3, top) or from the geometry difference (Fig. 3, bottom). These changes were not visible in the absorption spectrum and mainly concern modifications of some relative intensities. For example, the modes at about  $610\text{ cm}^{-1}$  ( $\nu_1$ ),  $770\text{ cm}^{-1}$ ,  $1350\text{ cm}^{-1}$  ( $\nu_2$ ), and  $1510\text{ cm}^{-1}$  ( $\nu_3$ ) have slightly larger RR intensities when using displacements calculated from the gradients (Fig. 3, top), whereas the vibration at about  $1650\text{ cm}^{-1}$  ( $\nu_4$ ) has a stronger intensity in the case of displacements calculated

from the geometry difference (Fig. 3, bottom). Comparison with the experimental spectrum (see Fig. 4) shows that the former spectrum (Fig. 3, top) is in slightly better agreement with the experimental results. Although the differences are relatively moderate, this seems to indicate that in this case, the displacements obtained from the vertical gradients are more accurate. A discussion of the respective merits of vertical and adiabatic models for the description of the potential energy surfaces as well as applications to different systems can be found, e.g., in Refs. 14, 26, 18, and 50.

The inclusion of Duschinsky effects mainly leads to an overall decrease of the absolute cross section, which can be related to the lower absorption cross section close to the maximum when including Duschinsky effects (Fig. 2, top) as well as to the incomplete convergence of the SOS expression. Some changes of relative RR intensities are also observed when considering Duschinsky effects, e.g., for the vibrations  $\nu_1$  and  $\nu_4$ , but generally they remain small. Therefore, in the case of the  $S_1$  state of R6G, it can be concluded that the IMDHO model provides an accurate description of the RR properties. Thus, in the following the impact of the FC/HT and HT, contributions will only be investigated using the IMDHO model.

The top-left of Fig. 4 describes the effects of FC/HT and HT contributions on the RR spectrum within the IMDHO

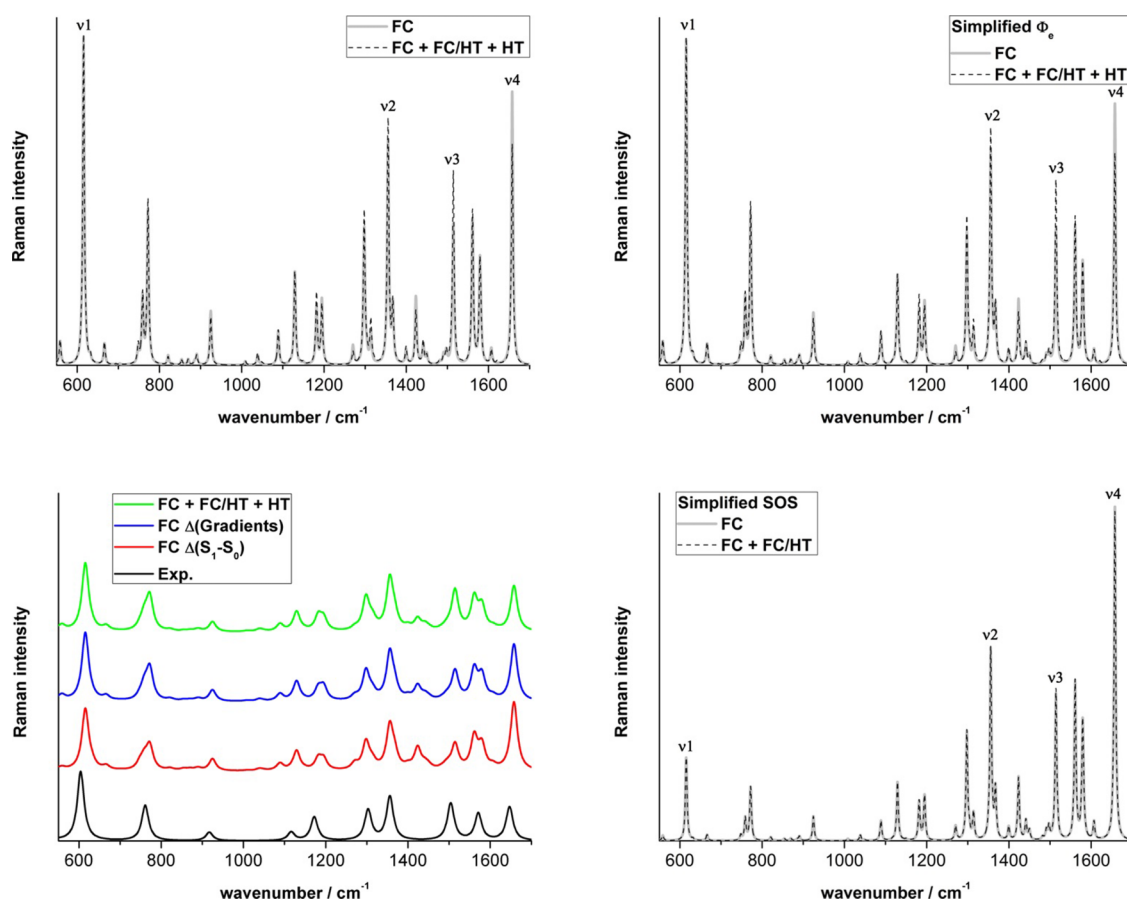


FIG. 4. Comparison between RR spectra obtained for an excitation in close resonance with the maximum of absorption. On the top-left (IMDHO model), top-right (simplified  $\Phi_e$ ), and bottom-right (simplified SOS), the spectra are calculated in the FC approximation (grey line) and including HT effects (dashed line) with  $\Delta$ 's obtained from the gradients. Bottom-left: Experimental spectrum<sup>52,32</sup> (black line), IMDHO model in the FC approximation with  $\Delta$ 's obtained from the difference between the  $S_1$  and  $S_0$  geometries (red line) and with  $\Delta$ 's obtained from the gradients (blue line), including HT effects (green line). In the calculated spectra, a Lorentzian function with a FWHM of  $20\text{ cm}^{-1}$  was employed to broaden the RR intensities.

model. Contrary to the absorption spectrum, the inclusion of HT effects leads to noticeable changes in several relative RR intensities. Similar effects were noticed in other systems (see, e.g., Refs. 25 and 50). This is mainly the case for the vibration  $\nu_3$ , which has a larger intensity when HT effects are included, and for the vibration  $\nu_4$ , for which HT effects leads to a decrease of the RR intensity. Interestingly, these modifications appear to improve the agreement with the experimental spectrum (see Fig. 4, bottom-left), which indicates that consideration of such contributions can be important even when in resonance with strongly allowed transitions.

The top-right of Fig. 4 presents the RR spectra obtained using the simplified  $\Phi_e$  approximation. Comparison with the spectra on the top-left of Fig. 4 clearly shows that the simplified  $\Phi_e$  method provides very similar results as the IMDHO model. This concerns both the FC and FC + FC/HT + HT approximations. In particular, the simplified  $\Phi_e$  method perfectly reproduces the strong intensities of the low frequency modes at about  $610\text{ cm}^{-1}$  ( $\nu_1$ ) and  $770\text{ cm}^{-1}$ , which are underestimated with the short-time approximation. Therefore, it is seen that neglecting the FC factors in the  $\Phi_e$  function (Eq. (16)) has only a minor effect on the relative RR intensities and that this approximation is adequate to reproduce the RR spectrum including both FC and HT effects. Investigation of the relative importance of the FC/HT and HT contributions (see Fig. S1<sup>36</sup>) demonstrates that the HT effects entirely originate from the FC/HT contribution, while the higher-order HT contribution is negligible in the present case.

The RR spectra calculated with the simplified SOS expression are reported on the bottom-right of Fig. 4. Two main observations can be made. First, the simplified SOS method fails in reproducing the large RR intensities of the two low frequency modes and provides a too large RR intensity for the vibration  $\nu_4$ . In fact, the spectrum obtained with the simplified SOS approach resembles closely the spectrum calculated with the short-time approximation (Fig. 3, top). Second, the effects of the FC/HT contribution are almost negligible using this approximation. Therefore, the results obtained with the simplified SOS method contrast strongly with the results calculated using the simplified  $\Phi_e$  function. However, this latter approach is in better agreement with the higher level methods (i.e., IMDHO model and full SOS) as well as with the experimental spectrum. Hence, the results show that the simplified SOS method is not fully adequate to simulate the RR intensities of R6G and does not provide a proper inclusion of the HT effects. Because both simplified SOS and simplified  $\Phi_e$  (using displacements calculated from the gradients) methods employ the same input data and require nearly identical computational cost, the simplified  $\Phi_e$  approximation should be preferred over the simplified SOS approach to calculate RR intensities.

### C. RR excitation profiles

In Sec. V B, the RR spectra were calculated assuming a fixed excitation frequency in close resonance with the absorption maximum. However, the RR cross sections and

relative RR intensities are dependent on the excitation frequency. These effects can be analyzed in detail by investigating the RR excitation profiles (RREPs). As a matter of illustration, the RREPs of the four most intense vibrations are computed and presented in Fig. 5.

The top of Fig. 5 shows the RREPs calculated within the IMDHO model including FC and HT effects. The RREPs display typical shapes in agreement with a previous work.<sup>32</sup> In particular, the RREP for the low frequency mode  $\nu_1$  is composed of a single band with a very weak shoulder at

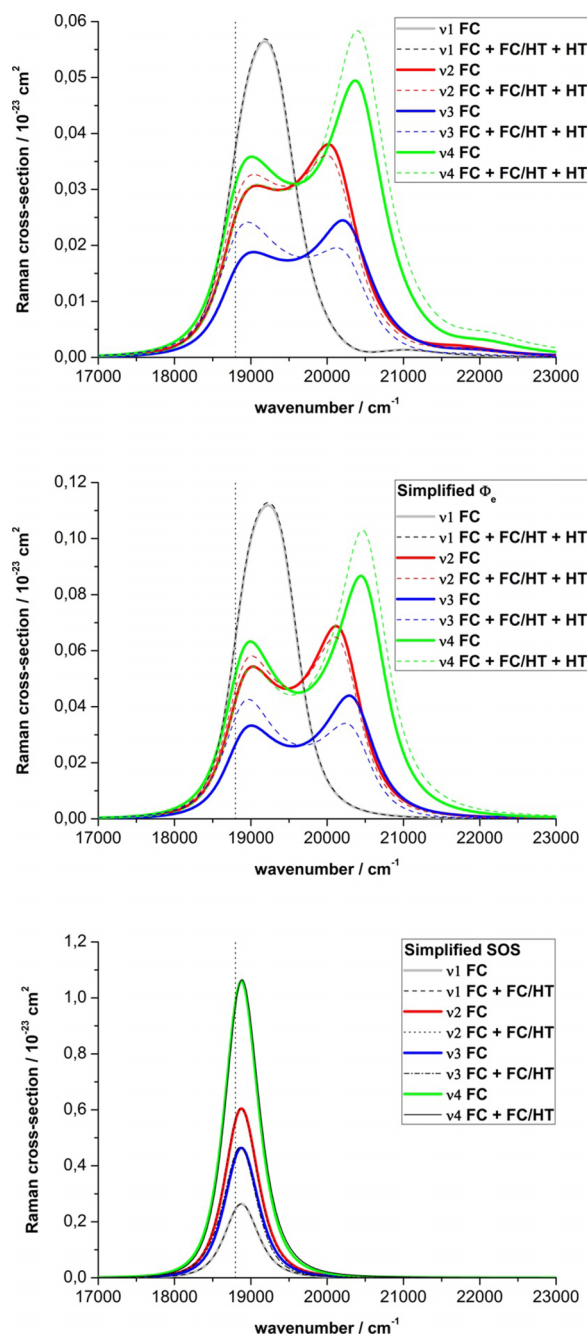


FIG. 5. Comparison between the RR excitation profiles of the four selected modes. On the top (IMDHO model), middle (simplified  $\Phi_e$ ), and bottom (simplified SOS) the profiles are calculated in the FC approximation (full lines) and including HT effects (dashed lines) with  $\Delta$ 's obtained from the gradients. The vertical dotted line indicates the excitation frequency employed in Section V B.

about  $21\,000\text{ cm}^{-1}$  originating from the vibronic structure (i.e., FC factors) in the  $\Phi_e$  function. However, the RREPs of the higher frequency modes  $\nu_2$ ,  $\nu_3$ , and  $\nu_4$  present a typical two bands shape, which highlights the strong dependence of the RR cross section with respect to the excitation frequency. The inclusion of the FC/HT and HT contributions shows that HT effects are negligible for the vibration  $\nu_1$ , whereas they are more important for the higher frequency modes. The importance of the HT effects is related to the magnitude of the derivative of the transition dipole moment  $(\mu_\rho)'_n$ . More precisely, the HT effects can lead to an enhancement or to a de-enhancement of the RR cross section depending on the considered mode and depending on the excitation frequency. For example, the intensities of the modes  $\nu_2$  and  $\nu_3$  are increased for an excitation close to the absorption maximum and decreased for an excitation at larger frequencies, i.e., above  $\sim 20\,000\text{ cm}^{-1}$ . However, it can be seen that the situation is opposite in the case of mode  $\nu_4$ . A detailed study of the different contributions shows that the HT effects originate from the first two terms in Eq. (15.2), namely,  $\mu_\rho(\mu_\sigma)'_n\Phi_e(\omega_L - \omega_n) + (\mu_\rho)'_n\mu_\sigma\Phi_e(\omega_L)$ , whereas the other terms lead to negligible contributions in the case of R6G (see Figs. S1 and S2<sup>36</sup>). The interference of this non-negligible contribution with the FC contribution (Eq. (15.1)) produces positive or negative corrections to the RR cross section around the two resonances in the RREP, which are centered at frequencies of about  $\omega_{eg}$  (first resonance) and  $\omega_{eg} + \omega_n$  (second resonance). In the present case, the differences between the behaviors of the modes  $\nu_2$  and  $\nu_3$  in comparison to the mode  $\nu_4$  stem from opposite signs for the values of the displacements  $\Delta_n$ , while  $\mu_\rho$  and  $(\mu_\rho)'_n$  have positive values.

The RREPs obtained with the simplified  $\Phi_e$  method are presented in the middle of Fig. 5. By comparing the results obtained with the IMDHO model (Fig. 5, top), it is seen that the simplified  $\Phi_e$  approach provides RREPs of comparable shapes and that the inclusion of HT effects is properly reproduced. In particular, this method is able to describe the two resonances present in the RREPs. Differences concern the absence of the weak vibronic shoulder above  $21\,000\text{ cm}^{-1}$  as well as some changes in the relative intensities at given excitation frequencies arising from the simplified shape of the  $\Phi_e$  function, i.e., neglect of the FC factors. Nevertheless, this shows that when the vibronic structure can be neglected, the simplified  $\Phi_e$  method provides an adequate formalism to calculate RR intensities at a low computational cost and including HT effects.

The full SOS approach including Duschinsky rotation effects was also applied including the FC contribution (see Fig. S3<sup>36</sup>). In agreement with the data presented in Sections V A and V B, these results show that the RREPs have comparable shapes as those obtained with the IMDHO model (Fig. 5, top).

The RREPs calculated with the simplified SOS approach are reported at the bottom of Fig. 5. The RREPs present a similar shape for all the modes and are composed of a single band centered at  $\Omega_{eg}$ . Indeed, the simplified SOS approach does not reproduce the second resonance located at higher frequencies (see Eq. (17) and supplementary material<sup>36</sup>) as

well as the vibronic structure described by the FC factors. Moreover, the HT effects are almost negligible in this case, which can be related to the overestimation of the FC contribution. The combination of these approximations leads to relative RR intensities showing no dependence with respect to the excitation frequency. In particular, the cross sections of the higher frequency modes are overestimated and the low frequency modes are not enhanced for an excitation close to the maximum of absorption. These results are in strong contrast to the results obtained with the simplified  $\Phi_e$  and higher-level methods (IMDHO model, full SOS) and indicate that the frequency dependence of the RREPs is not properly described using the simplified SOS method. Therefore, following the conclusion of Section V B, the simplified  $\Phi_e$  approximation should be preferred over the simplified SOS approach to calculate RR intensities.

The validity of the simplified  $\Phi_e$  method is further investigated in the frame of the FC approximation. The first column of Fig. 6 reproduces the absorption spectra and the RREPs obtained for R6G. In this case, the good agreement between the RREPs obtained with the simplified  $\Phi_e$  method and the IMDHO model can be related to the small values of the displacements. This leads to an absorption spectrum with a weak vibronic shoulder and to comparable values of the adiabatic  $\omega_{eg}$  ( $18\,800\text{ cm}^{-1}$ ) and vertical  $\Omega_{eg}$  ( $18\,867\text{ cm}^{-1}$ ) transition frequencies. In such a situation the simplified  $\Phi_e$  method is similar to the small shift approximation (see Section III C and the supplementary material<sup>36</sup>). To test the effects of larger shifts, all the displacements of R6G were multiplied by the factor 2.0 and the same adiabatic frequency ( $\omega_{eg}$ ) is employed. In this case, the absorption spectrum (Fig. 6, middle-top) in the IMDHO model displays a marked vibronic shoulder. This shoulder cannot be reproduced by the simplified  $\Phi_e$  method, but in order to approximate the broadening and to reproduce the position of the absorption maximum, values of  $800\text{ cm}^{-1}$  and of  $19\,225\text{ cm}^{-1}$  were used for the damping factor  $\Gamma$  and for the vertical frequency ( $\Omega_{eg}$ ), respectively (Fig. 6, middle column). The RREPs within the IMDHO model show complex shapes characterized by the presence of a vibronic structure. In this case, the simplified  $\Phi_e$  method presents only a partial agreement with the IMDHO model. In particular, the RREPs for excitations below  $\sim 20\,500\text{ cm}^{-1}$  are still adequately reproduced, but important deviations are obtained for larger excitation frequencies, which is related to the lack of vibronic structure in the simplified  $\Phi_e$  approach. Nevertheless, it is seen that the simplified  $\Phi_e$  method provides a better reproduction of the shape and position of the RREPs than the simplified SOS approach. The right column of Fig. 6 presents a situation in which the twice larger displacements are employed together with a larger broadening ( $\Gamma = 1500\text{ cm}^{-1}$ ). In this case, the details of the vibronic structure are hidden by the large broadening and it is seen that the IMDHO model and the simplified  $\Phi_e$  method provide globally comparable RREPs. The differences concern a small deviation between the RREP maxima and the fact that the IMDHO model gives broader RREPs due to the inclusion of the vibronic structure. Similarly in this case, the simplified  $\Phi_e$  method provides better results than the simplified SOS approach. Generally, it can be concluded that the simplified  $\Phi_e$  method gives a



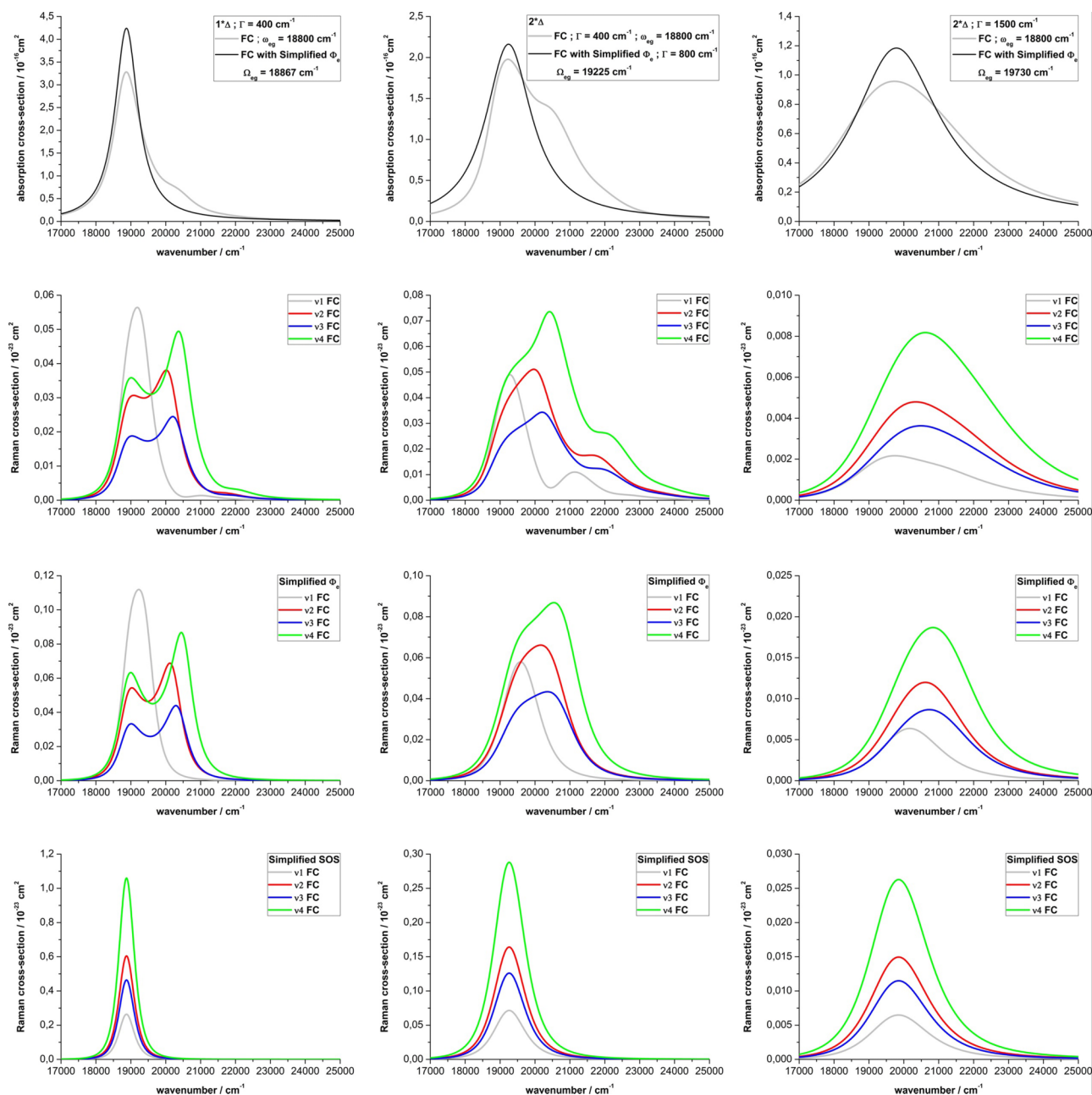


FIG. 6. Comparison between the absorption spectra and the RR excitation profiles in the FC approximation. The values of the  $\Delta$ 's obtained from the gradients are multiplied by 2 in the middle and right columns, and different values of the broadening are employed. The absorption spectra are given in the first row using the IMDHO model and the simplified  $\Phi_e$  approach, whereas the RR profiles are depicted in the second (IMDHO model), third (simplified  $\Phi_e$ ), and fourth (simplified SOS) rows.

correct reproduction of the RREPs obtained with the IMDHO model, provided the excitation frequency is in resonance with absorption bands displaying a large broadening and non-resolved vibronic structure, i.e., in situations in which the absorption band can be approximated by a simple Lorentzian function.

## VI. CONCLUSIONS

In the present work, SOS expressions to simulate the related spectroscopies of absorption and RR—including both FC and HT effects—have been described. Several approximations were summarized (Fig. 1), namely, the general

full SOS method, the IMDHO model, the simplified  $\Phi_e$  approach, the simplified SOS method, and the well-known short-time approximation. The most involved method is the full SOS, which allows, e.g., inclusion of Duschinsky rotation effects. In the case of the IMDHO model, practical expressions were derived, which only require the calculation of a given type of FC overlap integrals, i.e.,  $\langle \theta_{g0} | \theta_{ev} \rangle$ , making the method computationally advantageous. Within the latter approach, a straightforward simplification can be introduced in the  $\Phi_e$  function leading to the so-called simplified  $\Phi_e$  method. This simplification is justified in situations when the vibronic structure described by the FC factors can be neglected. Additionally, an expression reported recently in

the literature<sup>27</sup> and called herein the simplified SOS method has been presented. This method requires identical input data as the simplified  $\Phi_e$  approach and has therefore an identical computational cost.

As a matter of illustration, the different methods were applied to the prototypical compound of R6G. The impact of the different simplifications and of the HT effects on the absorption, RR spectra, and RREPs was described. Comparison with experimental results was also performed. It was found that (i) the excited state gradients provide an accurate evaluation of the geometrical displacements, (ii) the inclusion of HT effects is improving the RR intensities when comparing with the experimental results, (iii) the IMDHO model leads to comparable spectra as the more involved full SOS approach, (iv) the simplified  $\Phi_e$  method is adequate to reproduce the RR intensities of R6G, for which there is only a weak effect of the FC factors, and (v) the simplified SOS approach is less accurate than the simplified  $\Phi_e$  method and provides similar spectra as the short-time approximation. Because both simplified SOS and simplified  $\Phi_e$  (using displacements calculated from the gradients) methods employ the same input data and require nearly identical computational cost, the simplified  $\Phi_e$  approximation should be preferred over the simplified SOS method to calculate RR intensities.

In general, the IMDHO model and the simplified  $\Phi_e$  method appear to be good alternatives to the more involved full SOS approach due to their lower computational cost and their ability to properly include HT effects. These two approaches can also easily be implemented in any quantum chemistry program. Therefore, it is expected that they will be employed in the future—in conjunction with the full SOS method when necessary—to describe large molecular systems, in which the multimode character and the presence of several electronic excited states in resonance should be taken into account.

## ACKNOWLEDGMENTS

The author is grateful to the 7th Framework Programme of the European Union (Grant Agreement No. 321971) and to the Narodowe Centrum Nauki (Project No. 2014/14/M/ST4/00083) for financial support. The calculations have been performed at the Universitätsrechenzentrum of the Friedrich-Schiller University of Jena.

- <sup>1</sup>D. A. Long, *The Raman Effect: A Unified Treatment of the Theory of Raman Scattering by Molecules* (John Wiley & Sons Ltd, New York, 2002).  
<sup>2</sup>A. C. Albrecht, *J. Chem. Phys.* **34**, 1476 (1961).  
<sup>3</sup>M. Wächtler, J. Guthmuller, L. González, and B. Dietzek, *Coord. Chem. Rev.* **256**, 1479 (2012).  
<sup>4</sup>A. B. Myers, *Chem. Rev.* **96**, 911 (1996).  
<sup>5</sup>A. M. Kelley, *J. Phys. Chem. A* **112**, 11975 (2008).  
<sup>6</sup>R. Horvath and K. C. Gordon, *Coord. Chem. Rev.* **254**, 2505 (2010).  
<sup>7</sup>H. A. Kramers and W. Heisenberg, *Z. Phys.* **31**, 681 (1925).  
<sup>8</sup>P. A. M. Dirac, *Proc. R. Soc. A* **114**, 710 (1927).  
<sup>9</sup>E. J. Heller, R. L. Sundberg, and D. Tannor, *J. Phys. Chem.* **86**, 1822 (1982).  
<sup>10</sup>S.-Y. Lee and E. J. Heller, *J. Chem. Phys.* **71**, 4777 (1979).  
<sup>11</sup>A. B. Myers, R. A. Mathies, D. J. Tannor, and E. J. Heller, *J. Chem. Phys.* **77**, 3857 (1982).  
<sup>12</sup>D. J. Tannor and E. J. Heller, *J. Chem. Phys.* **77**, 202 (1982).  
<sup>13</sup>T. Petrenko and F. Neese, *J. Chem. Phys.* **127**, 164319 (2007).

- <sup>14</sup>T. Petrenko and F. Neese, *J. Chem. Phys.* **137**, 234107 (2012).  
<sup>15</sup>D. W. Silverstein and L. Jensen, *J. Chem. Phys.* **136**, 064111 (2012).  
<sup>16</sup>D. W. Silverstein, N. Govind, H. J. J. Van Dam, and L. Jensen, *J. Chem. Theory Comput.* **9**, 5490 (2013).  
<sup>17</sup>H. Ma, J. Liu, and W. Liang, *J. Chem. Theory Comput.* **8**, 4474 (2012).  
<sup>18</sup>A. Baiardi, J. Bloino, and V. Barone, *J. Chem. Phys.* **141**, 114108 (2014).  
<sup>19</sup>J. Guthmuller and B. Champagne, *J. Chem. Phys.* **127**, 164507 (2007).  
<sup>20</sup>J. Neugebauer and B. A. Hess, *J. Chem. Phys.* **120**, 11564 (2004).  
<sup>21</sup>K. A. Kane and L. Jensen, *J. Phys. Chem. C* **114**, 5540 (2010).  
<sup>22</sup>J. Romanova, V. Liégeois, and B. Champagne, *J. Phys. Chem. C* **118**, 12469 (2014).  
<sup>23</sup>J. Romanova, V. Liégeois, and B. Champagne, *Phys. Chem. Chem. Phys.* **16**, 21721 (2014).  
<sup>24</sup>F. Santoro, C. Cappelli, and V. Barone, *J. Chem. Theory Comput.* **7**, 1824 (2011).  
<sup>25</sup>F. J. A. Ferrer, V. Barone, C. Cappelli, and F. Santoro, *J. Chem. Theory Comput.* **9**, 3597 (2013).  
<sup>26</sup>F. Egidi, J. Bloino, C. Cappelli, and V. Barone, *J. Chem. Theory Comput.* **10**, 346 (2014).  
<sup>27</sup>D. Rappoport, S. Shim, and A. Aspuru-Guzik, *J. Phys. Chem. Lett.* **2**, 1254 (2011).  
<sup>28</sup>J. B. Cabalo, S. K. Saikin, E. D. Emmons, D. Rappoport, and A. Aspuru-Guzik, *J. Phys. Chem. A* **118**, 9675 (2014).  
<sup>29</sup>S. Kupfer, M. Wächtler, J. Guthmuller, J. Popp, B. Dietzek, and L. González, *J. Phys. Chem. C* **116**, 19968 (2012).  
<sup>30</sup>J. Guthmuller, B. Champagne, C. Moucheron, and A. Kirsch-De Mesmaeker, *J. Phys. Chem. B* **114**, 511 (2010).  
<sup>31</sup>J. Guthmuller and B. Champagne, *J. Phys. Chem. A* **112**, 3215 (2008).  
<sup>32</sup>J. Guthmuller and B. Champagne, *ChemPhysChem* **9**, 1667 (2008).  
<sup>33</sup>A. Warshel and P. Dauber, *J. Chem. Phys.* **66**, 5477 (1977).  
<sup>34</sup>F. Neese, T. Petrenko, D. Ganyushin, and G. Olbrich, *Coord. Chem. Rev.* **251**, 288 (2007).  
<sup>35</sup>F. Santoro, A. Lami, R. Improta, J. Bloino, and V. Barone, *J. Chem. Phys.* **128**, 224311 (2008).  
<sup>36</sup>See supplementary material at <http://dx.doi.org/10.1063/1.4941449> for details of the theoretical derivation and additional information on the RR intensities.  
<sup>37</sup>P. T. Ruhoff, *Chem. Phys.* **186**, 355 (1994).  
<sup>38</sup>J. Guthmuller, F. Zutterman, and B. Champagne, *J. Chem. Phys.* **131**, 154302 (2009).  
<sup>39</sup>C. Manneback, *Physica* **17**, 1001 (1951).  
<sup>40</sup>D. L. Tonks and J. B. Page, *Chem. Phys. Lett.* **66**, 449 (1979).  
<sup>41</sup>V. Hizhnyakov and I. Tehver, *Phys. Status Solidi B* **21**, 755 (1967).  
<sup>42</sup>D. C. Blazej and W. L. Peticolas, *J. Chem. Phys.* **72**, 3134 (1980).  
<sup>43</sup>W. L. Peticolas and T. Rush, *J. Comput. Chem.* **16**, 1261 (1995).  
<sup>44</sup>B. R. Stallard, P. M. Champion, P. R. Callis, and A. C. Albrecht, *J. Chem. Phys.* **78**, 712 (1983).  
<sup>45</sup>J. Guthmuller and L. González, *Phys. Chem. Chem. Phys.* **12**, 14812 (2010).  
<sup>46</sup>Y. Zhang, S. Kupfer, L. Zedler, J. Schindler, T. Bocklitz, J. Guthmuller, S. Rau, and B. Dietzek, *Phys. Chem. Chem. Phys.* **17**, 29637 (2015).  
<sup>47</sup>L. Jensen, L. L. Zhao, J. Autschbach, and G. C. Schatz, *J. Chem. Phys.* **123**, 174110 (2005).  
<sup>48</sup>A. Mohammed, H. Ågren, and P. Norman, *Chem. Phys. Lett.* **468**, 119 (2009).  
<sup>49</sup>A. Mohammed, H. Ågren, and P. Norman, *Phys. Chem. Chem. Phys.* **11**, 4539 (2009).  
<sup>50</sup>N. Lin, V. Barone, C. Cappelli, X. Zhao, K. Ruud, and F. Santoro, *Mol. Phys.* **111**, 1511 (2013).  
<sup>51</sup>M. J. Frisch, G. W. Trucks, H. B. Schlegel, G. E. Scuseria, M. A. Robb, J. R. Cheeseman, G. Scalmani, V. Barone, B. Mennucci, G. A. Petersson, H. Nakatsuji, M. Caricato, X. Li, H. P. Hratchian, A. F. Izmaylov, J. Bloino, G. Zheng, J. L. Sonnenberg, M. Hada, M. Ehara, K. Toyota, R. Fukuda, J. Hasegawa, M. Ishida, T. Nakajima, Y. Honda, O. Kitao, H. Nakai, T. Vreven, J. J. A. Montgomery, J. E. Peralta, F. Ogliaro, M. Bearpark, J. J. Heyd, E. Brothers, K. N. Kudin, V. N. Staroverov, R. Kobayashi, J. Normand, K. Raghavachari, A. Rendell, J. C. Burant, S. S. Iyengar, J. Tomasi, M. Cossi, N. Rega, J. M. Millam, M. Klene, J. E. Knox, J. B. Cross, V. Bakken, C. Adamo, J. Jaramillo, R. Gomperts, R. E. Stratmann, O. Yazyev, A. J. Austin, R. Cammi, C. Pomelli, J. W. Ochterski, R. L. Martin, K. Morokuma, V. G. Zakrzewski, G. A. Voth, P. Salvador, J. J. Dannenberg, S. Dapprich, A. D. Daniels, O. Farkas, J. B. Foresman, J. V. Ortiz, J. Cioslowski, and D. J. Fox, *GAUSSIAN 09*, Revision A.02 (Gaussian, Inc., Wallingford, CT, 2009).  
<sup>52</sup>S. Shim, C. M. Stuart, and R. A. Mathies, *ChemPhysChem* **9**, 697 (2008).